

# Preparation, Properties, and Crystal Structure of $Zr_5Zn_{39}$ , a Vacancy Variant of the $Ce_5Mg_{41}$ -Type, and Structure Refinement of $ZrZn_{22}$

Xue-an Chen<sup>1</sup> and Wolfgang Jeitschko<sup>2</sup>

*Anorganisch-Chemisches Institut, Universität Münster, Wilhelm-Klemm-Str. 8, D-48149 Münster, Germany*

Received June 5, 1995; accepted August 17, 1995

Well-developed crystals of  $Zr_5Zn_{39}$  and  $ZrZn_{22}$  were obtained from binary alloys with an excess of zinc by dissolving the matrices in hydrochloric acid, which attacks the binary compounds at a slower rate. Both compounds are diamagnetic with susceptibility values of  $\chi = -25(\pm 15) \times 10^{-9} \text{ m}^3/\text{mol}$  for  $Zr_5Zn_{39}$  and  $\chi = -12(\pm 2) \times 10^{-9} \text{ m}^3/\text{mol}$  for  $ZrZn_{22}$ . Electrical conductivity measurements confirm the expected metallic conductivity of  $Zr_5Zn_{39}$ . The crystal structure of  $Zr_5Zn_{39}$  was determined from single-crystal X-ray diffractometer data:  $C2/m$ ,  $a = 1785.5(7) \text{ pm}$ ,  $b = 859.6(2) \text{ pm}$ ,  $c = 1254.6(4) \text{ pm}$ ,  $\beta = 134.40(2)^\circ$ ,  $Z = 2$ ,  $R = 0.035$  for 1744 structure factors and 119 variable parameters. The previously reported structure of  $ZrZn_{22}$  is confirmed:  $Fd\bar{3}m$ ,  $a = 1410.5(1) \text{ pm}$ ,  $Z = 8$ ,  $R = 0.026$  for 248  $F$  values and 18 variables. Both compounds show significant deviations from the full occupancy for one zinc site, resulting in the exact compositions  $Zr_5Zn_{38.921(7)}$  and  $ZrZn_{21.798(7)}$ . Both structures contain relatively large voids, which are suited for the accommodation of interstitial atoms. It is suggested that these voids are filled with nonbonding electrons of the zinc atoms. This is supported by the existence of the tetragonal  $Ce_5Mg_{41}$  type structure, which may be regarded as a *translationengleiche* "filled-up" version of  $Zr_5Zn_{39}$ . © 1996 Academic Press, Inc.

## INTRODUCTION

The phase diagram of the binary system zirconium–zinc has been investigated by Chiotti and Kilp (1), who found six binary phases.  $ZrZn$  has a CsCl structure (2); the well-known ferromagnetic compound  $ZrZn_2$  is isotypic with  $MgCu_2$  (3, 4);  $ZrZn_3$  is reported to be dimorphic with a phase transition at  $910^\circ\text{C}$  (1). Both structures are as yet undetermined. The phase designated as " $ZrZn_6$ " (1) is identical to the compound  $Zr_5Zn_{39}$  of the present paper. And finally " $ZrZn_{14}$ " (1) has been found from single-crys-

tal Weissenberg data to crystallize with a  $Mg_3Cr_2Al_{18}$  type structure with the ideal composition  $ZrZn_{22}$  (5). This structure is confirmed by the present work.

## SAMPLE PREPARATION AND LATTICE CONSTANTS

Both  $Zr_5Zn_{39}$  and  $ZrZn_{22}$  are formed by peritectic reactions (1). We therefore prepared single crystals of these compounds from samples with higher zinc contents. Starting materials were powders of zirconium and zinc, and zinc granules, all with nominal purities greater than 99.9%. For the preparation of  $Zr_5Zn_{39}$ , microcrystalline samples with the composition  $Zr:Zn = 1:3$  were first prepared by reaction of cold-pressed pellets at  $620^\circ\text{C}$  for one week with one intermittent grinding. The resulting products were mixed with granules of zinc in the atomic ratio  $Zr:Zn = 3.6:96.4$  and placed in alumina containers, which were sealed in silica tubes under argon. The samples were heated gradually to  $910^\circ\text{C}$ , where they were kept for six days, then cooled at a rate of  $5^\circ\text{C}/\text{h}$  to  $570^\circ\text{C}$ . They were annealed at that temperature for one day and quenched in water. The zinc-rich matrix was dissolved in diluted hydrochloric acid. This acid also attacks the crystals of  $Zr_5Zn_{39}$ , albeit at a slower rate. The crystals of  $Zr_5Zn_{39}$  had the shape of prisms with dimensions of up to  $0.2 \times 0.2 \times 2.0 \text{ mm}^3$ .

The crystals of  $ZrZn_{22}$  were prepared in the same way, except that the atomic starting ratio was  $Zr:Zn = 3.3:96.7$  and the slow cooling was extended to  $540^\circ\text{C}$ . After dissolving the zinc-rich matrix in hydrochloric acid two kinds of  $ZrZn_{22}$  crystals with diameters of up to 0.2 mm were observed. One kind had octahedral habit and these crystals proved to be real cubic single crystals. The other crystals had the form of triangular platelets. Their reciprocal lattice—recorded on the four-circle diffractometer—mimicked hexagonal symmetry  $6/mmm$ . The pseudohexagonal lattice constants ( $h$ ) of these crystals may be obtained from the cubic lattice constants ( $c$ ) by the relations  $a_h = a_c/\sqrt{2} = 997.4 \text{ pm}$  and  $c_h = a_c\sqrt{3} = 2443.1 \text{ pm}$ . These relationships suggest twinning with the cubic [111]

<sup>1</sup> Permanent address: Institute of Chemistry, Academia Sinica, Beijing 100080, P.R. China.

<sup>2</sup> To whom correspondence should be addressed.

TABLE 1  
Some Data and Results of the Structure Determinations of  $Zr_5Zn_{39-x}$  and  $ZrZn_{22-x}$ <sup>a</sup>

Structure type	$Zr_5Zn_{39}$	$Mg_3Cr_2Al_{18}$
Composition	$Zr_5Zn_{38.921(7)}$	$ZrZn_{21.798(7)}$
Crystal dimensions, $\mu m^3$	$30 \times 30 \times 80$	$50 \times 50 \times 50$
Space group	C2/m (No. 12)	Fd $\bar{3}m$ (No. 227)
Lattice constants from powder data		
<i>a</i> (pm)	1785.5(7)	1410.5(1)
<i>b</i> (pm)	859.6(2)	—
<i>c</i> (pm)	1254.6(4)	—
$\beta$	134.40(2) $^\circ$	—
<i>V</i> (nm <sup>3</sup> )	1.3758	2.8062
Lattice constants from single crystal data		
<i>a</i> (pm)	[1785.6(2)]	[1409.1(2)]
<i>b</i> (pm)	[860.8(1)]	—
<i>c</i> (pm)	[1253.0(2)]	—
$\beta$	[134.47(1) $^\circ$ ]	—
<i>V</i> (nm <sup>3</sup> )	[1.3744]	[2.7979]
Formula units/cell	<i>Z</i> = 2	<i>Z</i> = 8
Formula mass	3000.8	1516.4
Calculated density (g/cm <sup>3</sup> )	$\rho = 7.24$	$\rho = 7.18$
$\theta/2\theta$ scans up to	$2\theta = 75^\circ$	$2\theta = 85^\circ$
Range in <i>hkl</i>	$\pm 30, 0-14, \pm 21$	$0-26, 0-26, \pm 26$
Total number of reflections	7692	5292
Unique reflections	3924	566
Inner residual	$R_i = 0.034$	$R_i = 0.050$
Reflections with $I > n\sigma(I)$	1744 ( $n = 2$ )	248 ( $n = 1$ )
Highest/lowest transmission	1.09	1.11
Number of variables	119	18
Secondary extinction coefficient	$6.8 \times 10^{-8}$	$3.0 \times 10^{-7}$
Conventional residual	$R = 0.035$	$R = 0.026$
Weighted residual	$R_w = 0.035$	$R_w = 0.016$

<sup>a</sup> Standard deviations in the positions of the least significant digits are given in parentheses throughout the paper.

axis as the common twin axis, where the two domain orientations can be transformed into each other by a rotation of 60 $^\circ$  around the pseudohexagonal twin axis.

The crystals of  $Zr_5Zn_{39}$  and  $ZrZn_{22}$  are gray with metallic luster. They are stable in air for long periods of time but are slowly attacked by diluted hydrochloric acid. Energy-dispersive X-ray fluorescence analyses in a scanning electron microscope did not reveal any impurity elements heavier than sodium.

The lattice constants of  $Zr_5Zn_{39}$  and  $ZrZn_{22}$  were obtained from powder samples, which were prepared by annealing cold-pressed pellets of the elemental components with the ideal compositions at 360 $^\circ$ C for two weeks. The Guinier powder patterns were standardized with  $\alpha$ -quartz ( $a = 491.30$  pm,  $c = 540.46$  pm), and the lattice constants (Table 1) were obtained by least-squares fits of these data.

## PHYSICAL PROPERTIES

The electrical conductivity of a single crystal of  $Zr_5Zn_{39}$  was measured with a four-probe technique in the temperature range from 2 K to room temperature. A crystal of

about  $0.2 \times 0.2 \times 1.0$  mm<sup>3</sup> was contacted with four copper filaments using a well-conducting silver epoxy cement. A constant alternating current was maintained between two contacts and the voltage difference was measured by the other two contacts. Because of the uncertainties in estimating the size of the contacted areas, the absolute values of the electrical resistivities are estimated to be accurate only within a factor of three, however, the relative values at different temperatures are much more reliable. The resistivity increases with temperature (Fig. 1), indicating the expected metallic behavior. The room-temperature resistivity of  $Zr_5Zn_{39}$  is approximately  $\rho = 13 \mu\Omega$  cm, which is comparable to the literature values (6) of zinc ( $\rho = 5.9 \mu\Omega$  cm) and zirconium ( $\rho = 42 \mu\Omega$  cm).

Selected single crystals of  $Zr_5Zn_{39}$  and  $ZrZn_{22}$  were investigated with a SQUID magnetometer in the temperature range between 2 and 300 K at magnetic flux densities of up to 5.5 T. The magnetic susceptibility values of  $Zr_5Zn_{39}$  show relatively large scatter, because only five small crystals were used for this measurement. Both compounds show nearly temperature-independent diamagnetism at temperatures above 100 K (Fig. 2). The upturns at low

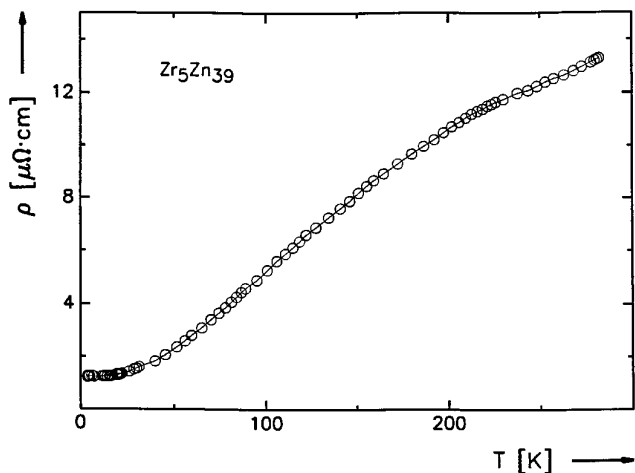


FIG. 1. Electrical resistivity of Zr<sub>5</sub>Zn<sub>39</sub> as a function of temperature.

temperatures and the field-dependence of the Zr<sub>5</sub>Zn<sub>39</sub> sample may be ascribed to minor amounts of para- and ferromagnetic impurities, respectively. Zr<sub>5</sub>Zn<sub>39</sub> was shown to be a metallic conductor and this is also expected for ZrZn<sub>22</sub>. Thus, temperature-independent Pauli paramagnetism can be assumed for both compounds. The negative values of the susceptibilities of  $\chi = -25(\pm 15) \times 10^{-9} \text{ m}^3/\text{formula unit}$  for Zr<sub>5</sub>Zn<sub>39</sub> and  $\chi = -12(\pm 2) \times 10^{-9} \text{ m}^3/\text{formula unit}$  for ZrZn<sub>22</sub> indicate that the Pauli paramagnetism is overcompensated by the core diamagnetism of the compounds.

### STRUCTURE DETERMINATIONS

Single crystals of both compounds were examined in Buerger precession cameras to establish their symmetry. The diffraction patterns of Zr<sub>5</sub>Zn<sub>39</sub> showed a *C*-centered monoclinic cell. The only systematic extinctions (reflections *hkl* were observed only with  $h + k = 2n$ ) were compatible with the space groups *C2*, *Cm*, and *C2/m*, of which the centrosymmetric group *C2/m* was found to be correct during the structure refinement. The precession photographs of ZrZn<sub>22</sub> confirmed the previously reported cubic *Fd* $\bar{3}m$  symmetry (5).

The X-ray diffraction intensity data for both compounds were recorded on an automated four-circle diffractometer with graphite-monochromated MoK $\alpha$  radiation and a scintillation counter with pulse-height discrimination. The background was determined on both sides of each  $\theta/2\theta$  scan. Empirical absorption corrections were made on the basis of psi-scan data. The crystallographic data and some results are summarized in Table 1.

The structure of Zr<sub>5</sub>Zn<sub>39</sub> was solved by direct methods with the SHELXS-86 (7) program system. For the refinement of the ZrZn<sub>22</sub> structure the positional parameters

were taken from the previous structure determination (5). A full-matrix least-squares program of the SDP package (8) was used for both structure refinements with atomic scattering factors (9), corrected for anomalous dispersion (10). The weighting schemes included a term, which accounted for the counting statistics and both data sets were corrected for isotropic secondary extinction by least-squares fits of one parameter. To check for deviations from the ideal compositions all occupancy parameters were allowed to vary along with the thermal parameters, while the scale factors were held constant. The resulting occupancies varied between the values of 0.983(5) for Zn10 and 1.017(3) for Zn6 in Zr<sub>5</sub>Zn<sub>39</sub> and between 1.001(4) for Zr and 1.017(4) for Zn4 in ZrZn<sub>22</sub>. The only exceptions were the Zn14 position of Zr<sub>5</sub>Zn<sub>39</sub> and the Zn3 position of ZrZn<sub>22</sub>, which showed significant deviations from the full occupancies with the occupancy values of 0.911(7) and 0.899(4), respectively. Therefore, in the final least-squares cycles all positions were assumed to be fully occupied with the exception of these two positions. Both sites were finally

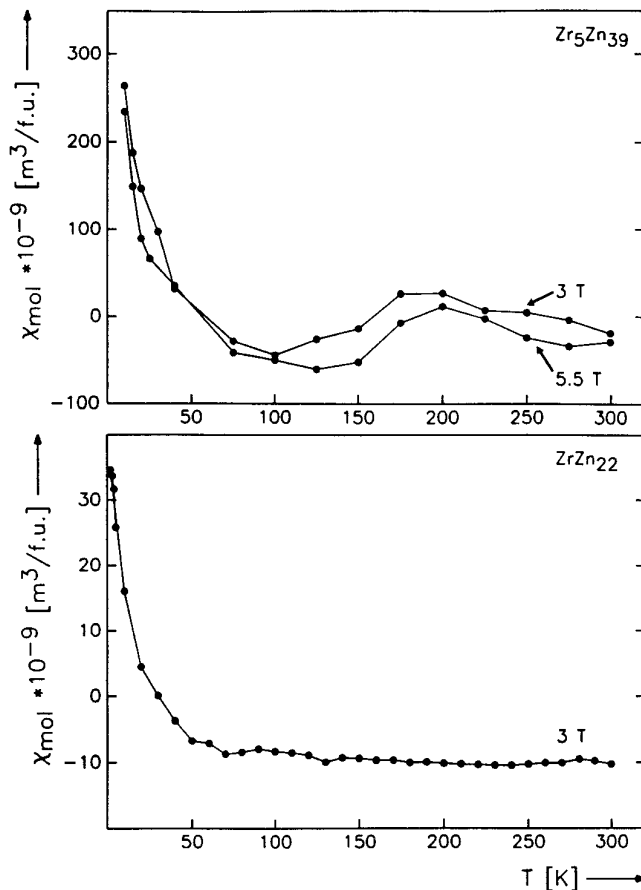


FIG. 2. Magnetic susceptibilities of Zr<sub>5</sub>Zn<sub>39</sub> and ZrZn<sub>22</sub> recorded with magnetic flux densities of 3 and 5.5 T. The upturns at low temperatures are ascribed to paramagnetic impurities. The lines connecting the data points are solely guides for the eye.

TABLE 2  
Atomic Parameters of  $Zr_5Zn_{39}$  and  $ZrZn_{22}$ <sup>a</sup>

Atom		x	y	z	$B_{eq}$
<b><math>Zr_5Zn_{38.921(7)}</math> (C2/m)</b>					
Zr1	4i	0.22798(6)	0	0.65234(9)	0.40(2)
Zr2	4i	0.42741(6)	0	0.20891(9)	0.45(2)
Zr3	2a	0	0	0	0.75(3)
Zn1	8j	0.07213(6)	0.3400(2)	0.19903(9)	0.97(2)
Zn2	8j	0.07543(6)	0.2390(1)	0.44328(8)	0.81(2)
Zn3	8j	0.12262(6)	0.3433(2)	0.04946(8)	0.98(2)
Zn4	8j	0.21617(6)	0.1552(1)	0.27116(8)	0.82(2)
Zn5	8j	0.37215(6)	0.2659(1)	0.29648(8)	0.86(2)
Zn6	8j	0.44272(6)	0.3464(1)	0.16227(8)	0.79(2)
Zn7	4i	0.12123(8)	0	0.3402(1)	0.76(3)
Zn8	4i	0.21557(9)	0	0.0925(1)	0.84(3)
Zn9	4i	0.34467(8)	0	0.5595(1)	0.68(3)
Zn10	4i	0.40460(9)	0	0.4211(1)	1.03(3)
Zn11	4i	0.78041(8)	0	0.1229(1)	0.73(3)
Zn12	4f	1/4	1/4	1/2	0.74(2)
Zn13	4e	1/4	1/4	0	0.81(3)
Zn14(92.1(7)% Zn)	2c	0	0	1/2	1.18(5)
<b><math>ZrZn_{21.798(7)}</math> (Fd<math>\bar{3}m</math>)</b>					
Zr	8a	1/8	1/8	1/8	0.336(5)
Zn1	96g	0.06174(3)	x	0.31920(4)	1.244(6)
Zn2	48f	0.48669(5)	1/8	1/8	1.011(8)
Zn3(89.9(4)% Zn)	16d	1/2	1/2	1/2	0.874(6)
Zn4	16c	0	0	0	1.361(6)

<sup>a</sup> The last column contains the equivalent isotropic  $B$  values in units of  $10^{-2}$  nm<sup>2</sup>. The Zn14 position of  $Zr_5Zn_{39}$  and the Zn3 position of  $ZrZn_{22}$  were found to be partially occupied. Both sites were finally refined to occupancies of 92.1(7) and 89.9(4)%, respectively. The atom labels Zr, Zn1–Zn4 of the presently reported standard setting of  $ZrZn_{22}$  (with the origin at the center of symmetry), correspond to the labels  $Zr_b$ ,  $Zn_g$ ,  $Zn_f$ ,  $Zn_c$ , and  $Zn_d$  of the earlier work (5); note that the sites 16c and 16d are interchanged.

refined to occupancies of 92.1(7) and 89.9(4)%, respectively. Thus the exact compositions of the crystals used for the structure determinations are  $Zr_5Zn_{38.921(7)}$  and  $ZrZn_{21.798(7)}$ . Final difference Fourier syntheses showed the highest electron densities of 2.9 and 0.4 e/Å<sup>3</sup> for  $Zr_5Zn_{39}$  and  $ZrZn_{22}$ . These values are rather small and furthermore they were too close to zinc positions to be suitable for the accommodation of any additional atoms. The conventional residuals (on F values) are listed in Table 1. The positional parameters (Table 2) are in the form standardized by the program STRUCTURE TIDY (11). Tables with the anisotropic thermal parameters and the structure factors are available from the authors.

## DISCUSSION

Before we start to discuss the new structure type of  $Zr_5Zn_{39}$  we will briefly comment on the structure refinement of  $ZrZn_{22}$ . This compound was found to be isotypic with  $Mg_3Cr_2Al_{18}$  (5, 12) by Samson, who described this structure in one of several papers on intermetallic com-

pounds with very large cells (13–16). Our present structure refinement fully confirms the earlier structure determination from Weissenberg data, which had resulted in a residual of 12%. The major remarkable difference lies in the occupancy of the 16c (Zn3) position, which earlier was assumed to be fully occupied, while our diffractometer data resulted in an occupancy of 89.9(4)%, assuming its occupancy solely by zinc atoms. This assumption is justified, since that site has the small coordination number 12 and it has six zinc neighbors at the distance of 250.1 pm, which is much shorter than the shortest Zr–Zn distances of 290.8 pm in  $Zr_5Zn_{39}$  and 301.6 pm in  $ZrZn_{22}$ .

In the earlier work (5) the possibility was discussed that the site  $Zn_d$  of  $ZrZn_{22}$  with the coordination number 14 (which corresponds to the Zn4 site of the presently used standardized setting) might have a mixed occupancy of zinc and zirconium. Our refinement of this occupation factor resulted in a value of 101.7(4)%, assuming an occupancy solely by zinc atoms. This value is only four standard deviations off the ideal occupancy and there is no need to refine this position with a mixed occupancy. Samson had consid-

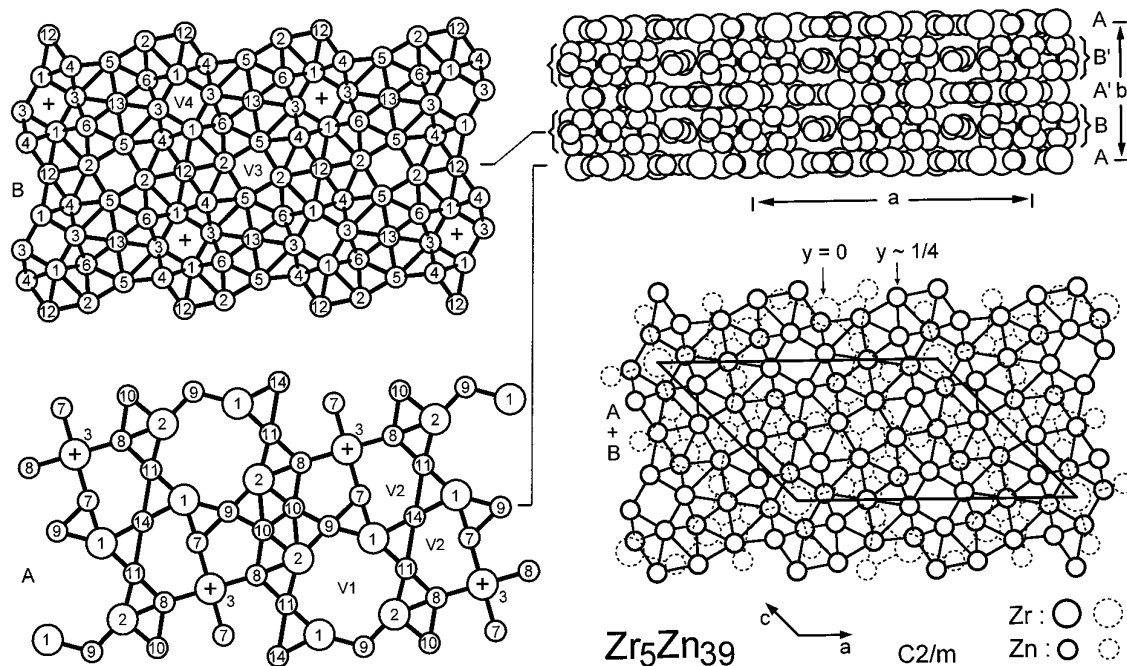


FIG. 3. Crystal structure of Zr<sub>5</sub>Zn<sub>39</sub>. The whole structure is shown in a projection along a direction perpendicular to the *ab* plane in the upper right-hand corner. Two kind of atomic layers can be discerned. The layers **A** are situated on the mirror plane of the *C2/m* cell. The layers **B** are puckered. A superposition of these two layers (at  $y = 0$  and  $y \sim 1/4$ ) projected along the *b* axis is shown below, and both layers are shown separately in the left-hand part of the figure, where the origin of the cell and the atom designations are indicated by crosses and numbers, respectively. Some positions of the voids V1 and V2 (at  $y = 0$ ) as well as V3 and V4 (at  $y \sim 1/4$ ) are also shown.

ered a mixed occupancy for that site, because the composition of his single-phase material was found by two laboratories to correspond to ZrZn<sub>20.4</sub> and ZrZn<sub>21.8</sub>, respectively. The latter is very close to the composition ZrZn<sub>21.798(7)</sub> found in the present refinement, assuming that the Zn3 position is only (partially) occupied by zinc atoms.

The structures of Zr<sub>5</sub>Zn<sub>39</sub> and ZrZn<sub>22</sub> with 88 and 184 atoms in their respective cells are not easy to visualize. In Figs. 3 and 4 we have chosen a description emphasizing atomic layers. One has to keep in mind, however, that the chemical bonding within and between the layers is of the same character. There are no preferred cleavage planes. The structure of Zr<sub>5</sub>Zn<sub>39</sub> may be regarded as being built up by the layers **A** and **B** (Fig. 3). The layers **A** are situated on the mirror plane of this monoclinic (*C2/m*) structure and therefore they are completely flat. In contrast, the layers **B** are puckered. They are densely populated by zinc atoms, whereas the layers **A** are less densely populated by both the zirconium and the zinc atoms. This building principle (sequences of densely and less densely populated layers) was also recognized in the structures of Ti<sub>3</sub>Zn<sub>22</sub> and TiZn<sub>16</sub> (17), but the layers themselves are always different. Four layers, **ABA'B'**, are needed to complete one translation period along the twofold axis of the Zr<sub>5</sub>Zn<sub>39</sub> structure. The layers **A** and **A'** as well as **B** and **B'** are identical,

however, because of the *C* centering, they are shifted relative to each other by half a translation period of the *a* direction, when viewed along the *b* direction.

The structure of ZrZn<sub>22</sub> can also be viewed as a layer structure. The layers extend perpendicular to the face diagonals of the cubic cell (Fig. 4). The layers **A** and **A'** are perfectly planar, because they correspond to mirror planes, whereas the other layers are slightly (almost invisibly) puckered. None of the layers are densely populated, and only the layers **A** (and **A'**) contain zirconium atoms.

In both structures all atoms have high coordination numbers (Table 3, Fig. 5). In ZrZn<sub>22</sub> the zirconium atoms have the coordination number (CN) 16 with the point symmetry  $\bar{4}3m$ . Thus, this is a perfect Frank-Kasper polyhedron (18, 19). The average Zr-Zn distance of 302.5 pm in this polyhedron is similar to the average Zr1-Zn distance of 300.2 pm of the Zr1 atom in Zr<sub>5</sub>Zn<sub>39</sub>, which also has CN 16, albeit with a much lower symmetry. The Zr2 and Zr3 atoms of Zr<sub>5</sub>Zn<sub>39</sub> have CN 17 and CN 20. Their average Zr-Zn distances of 305.6 pm and 327.0 pm reflect the higher CNs.

There are 14 different zinc sites in the structure of Zr<sub>5</sub>Zn<sub>39</sub> with CNs varying between 11 (Zn6 and Zn10) and 14 (Zn8). Each zinc atom has two or three zirconium neighbors. The average Zn-Zn distances vary between 267.7 pm for Zn6 (with CN 11) and 287.0 pm for Zn8 (with

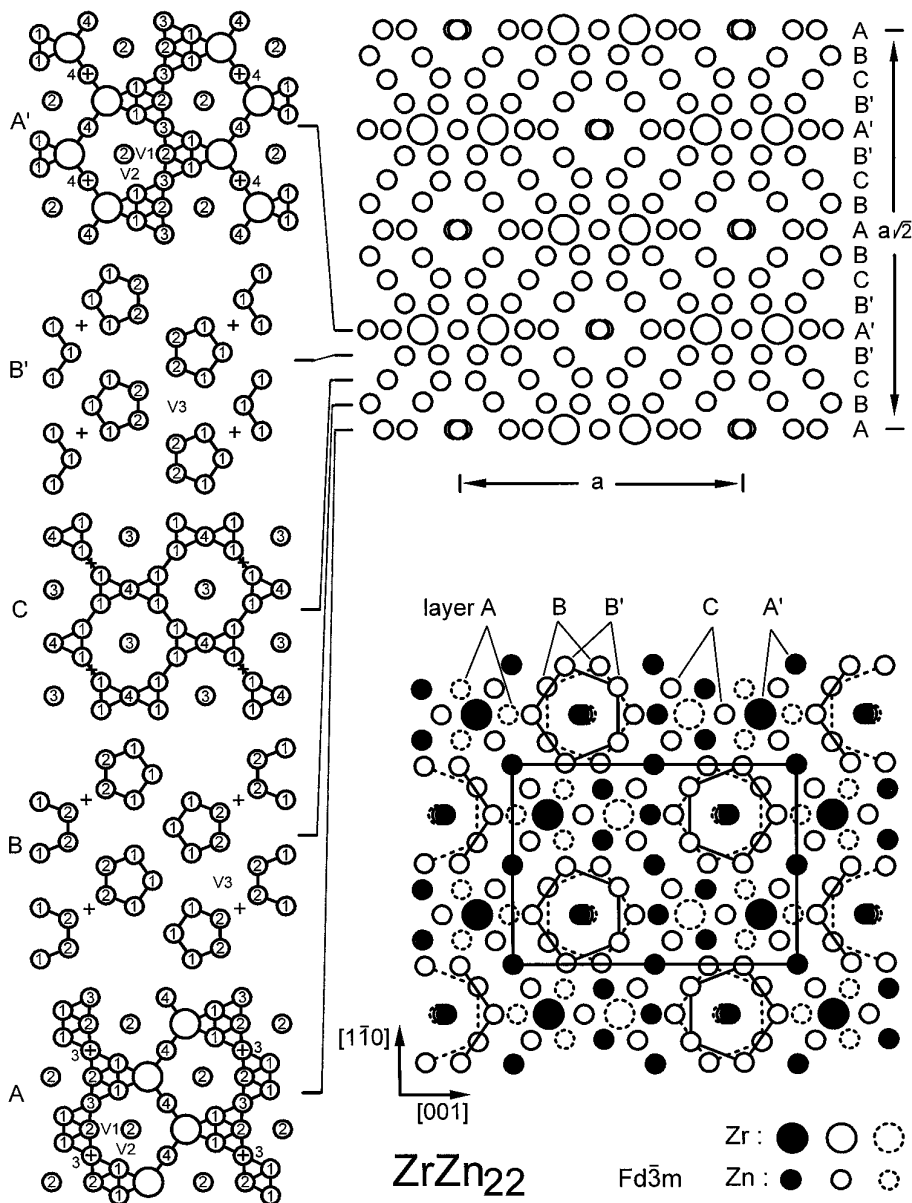


FIG. 4. Crystal structure of  $\text{ZrZn}_{22}$ . Atoms may be visualized as situated on the planes **A**, **B**, **C**, **B'**, **A'**. The layers extend perpendicular to the twofold axis, which are parallel to the  $\langle 110 \rangle$  directions of the cubic cell. These layers are shown separately (at a slightly reduced scale) on the left side and superimposed at the lower right-hand corner of the figure. Some positions of the large unoccupied interstitial sites V1–V3 are indicated. Single-digit numbers and crosses correspond to the atom designations and the origin positions of the cell.

CN 14). The only exception is the coordination polyhedron of the Zn14 atom, which has two zinc neighbors at the rather large distance of 343.5 pm. With these two neighbors the average Zn14–Zn distance is 291.5 pm; without them the CN decreases to 10 with an average Zn14–Zn distance 278.4 pm. This zinc position is also exceptional because it has an occupancy of only 92.1(7)%. In  $\text{ZrZn}_{22}$  there are only four zinc positions with coordination numbers of 12 (Zn1–Zn3) and 14 (Zn4). The Zn1 and Zn4 atoms have one and two zirconium neighbors, the others have none.

In both structures there are rather short Zn–Zn distances of 246.7 pm (Zn10–Zn10), 247.4 pm (Zn11–Zn13), 250.3 pm (Zn9–Zn12) in  $\text{Zr}_5\text{Zn}_{39}$ , and 250.1 pm (Zn2–Zn3) in  $\text{ZrZn}_{22}$ . Similar short Zn–Zn distances were observed in  $\text{Ti}_3\text{Zn}_{22}$  (17) with 244.1(2) pm and  $\text{NbZn}_2$  (20) with 245 pm.

In our discussion of the compounds  $\text{Ti}_3\text{Zn}_{22}$  and  $\text{TiZn}_{16}$  we have pointed out that these structures contain relatively large voids, which are big enough to accommodate additional small (“interstitial”) atoms like carbon, nitrogen, or oxygen (17). Such voids are also present in the structures

TABLE 3  
Interatomic Distances in Zr<sub>5</sub>Zn<sub>39</sub> and ZrZn<sub>22</sub><sup>a</sup>

<b>Zr<sub>5</sub>Zn<sub>39</sub></b>			
Zr1:	2Zn2	292.0	Zn2: 1Zr1 292.0
	1Zn7	292.0	1Zr2 312.9
	1Zn11	292.6	1Zn6 262.6
	2Zn1	296.5	1Zn12 267.0
	2Zn3	299.4	1Zn9 267.2
	1Zn9	301.5	1Zn10 268.4
	2Zn5	304.4	1Zn5 268.6
	1Zn14	305.6	1Zn5 269.5
	2Zn4	305.9	1Zn14 280.8
	2Zn12	307.9	1Zn7 283.6
Zr2:	1Zn9	290.8	1Zn4 297.5
	1Zn8	295.1	1Zn1 314.6
	1Zn10	296.1	Zn3: 1Zr1 299.4
	2Zn5	298.7	1Zr2 301.1
	2Zn1	300.5	1Zr3 346.2
	2Zn3	301.1	1Zn4 257.6
	1Zn11	308.0	1Zn1 257.7
	2Zn6	308.3	1Zn1 258.9
	2Zn2	312.9	1Zn6 259.6
	2Zn13	314.7	1Zn11 264.0
	1Zn10	332.6	1Zn3 269.5
Zr3:	4Zn6	313.8	1Zn13 285.9
	4Zn4	314.3	1Zn8 324.0
	2Zn8	314.8	1Zn5 325.2
	2Zn7	315.8	Zn4: 1Zr1 305.9
	4Zn1	345.5	1Zr3 314.3
	4Zn3	346.2	1Zn3 257.6
Zn1:	1Zr1	296.5	1Zn1 258.8
	1Zr2	300.5	1Zn8 260.3
	1Zr3	345.5	1Zn12 261.6
	1Zn6	257.4	1Zn4 266.9
	1Zn3	257.7	1Zn7 273.1
	1Zn4	258.8	1Zn5 274.3
	1Zn3	258.9	1Zn10 279.0
	1Zn9	264.1	1Zn9 291.9
	1Zn1	275.0	1Zn2 297.5
	1Zn12	285.7	
	1Zn2	314.6	
	1Zn7	320.6	
			Zn5: 1Zr2 298.7
			1Zr1 304.4
			1Zn11 254.6
			1Zn10 259.5
			1Zn2 268.6
			1Zn13 269.4
			1Zn2 269.5
			1Zn4 274.3
			1Zn14 276.1
			1Zn6 280.5
			1Zn8 309.5
			1Zn3 325.2
			Zn6: 1Zr2 308.3
			1Zr3 313.8
			1Zn1 257.4
			1Zn3 259.6
			1Zn13 262.1
			1Zn2 262.6
			1Zn7 263.3
			1Zn6 264.2
			1Zn8 270.3
			1Zn5 280.5
			1Zn11 289.6
			Zn7: 1Zr1 292.0
			1Zr3 315.8
			2Zn6 263.3
			2Zn4 273.1
			2Zn12 273.4
			2Zn2 283.6
			1Zn9 285.1
			2Zn1 320.6
			Zn8: 1Zr2 295.1
			1Zr3 314.8
			2Zn4 260.3
			2Zn6 270.3
			2Zn13 270.9
			1Zn11 275.3
			1Zn10 298.6
			2Zn5 309.5
			2Zn3 324.0
			Zn9: 1Zr2 290.8
			1Zr1 301.5
			2Zn12 250.3
			1Zn10 260.1
			2Zn1 264.1
			2Zn2 267.2
			1Zn7 285.1
			2Zn4 291.9
			Zn10: 1Zr2 296.1
			1Zr2 332.6
			1Zn10 246.7
			2Zn5 259.5
			1Zn9 260.1
			2Zn2 268.4
			2Zn4 279.0
			1Zn8 298.6
			Zn11: 1Zr1 292.6
			1Zr2 308.0
			2Zn13 247.4
			2Zn5 254.6
			2Zn3 264.0
			1Zn8 275.3
			2Zn6 289.6
			1Zn14 343.5
			Zn12: 2Zr1 307.9
			2Zn9 250.3
			2Zn4 261.6
			2Zn2 267.0
			2Zn7 273.4
			2Zn1 285.7
			Zn13: 2Zr2 314.7
			2Zn11 247.4
			2Zn6 262.1
			2Zn5 269.4
			2Zn8 270.9
			2Zn3 285.9
			Zn14: 2Zr1 305.6
			4Zn5 276.1
			4Zn2 280.8
			2Zn11 343.5
<b>ZrZn<sub>22</sub></b>			
Zr:	12Zn1	301.6	Zn1: 1Zr 301.6
	4Zn4	305.4	1Zn1 252.4
			2Zn1 261.2
			1Zn2 267.8
			1Zn3 283.2
			2Zn2 283.3
			2Zn1 294.5
			2Zn4 296.0
			Zn2: 2Zn3 250.1
			2Zn1 267.8
			4Zn2 275.9
			4Zn1 283.3
			Zn3: 6Zn2 250.1
			6Zn1 283.2
			Zn4: 2Zr 305.4
			12Zn1 296.0

<sup>a</sup> All distances shorter than 360 pm are given. All standard deviations are 0.2 pm or less in Zr<sub>5</sub>Zn<sub>39</sub> and less than 0.1 pm in ZrZn<sub>22</sub>.

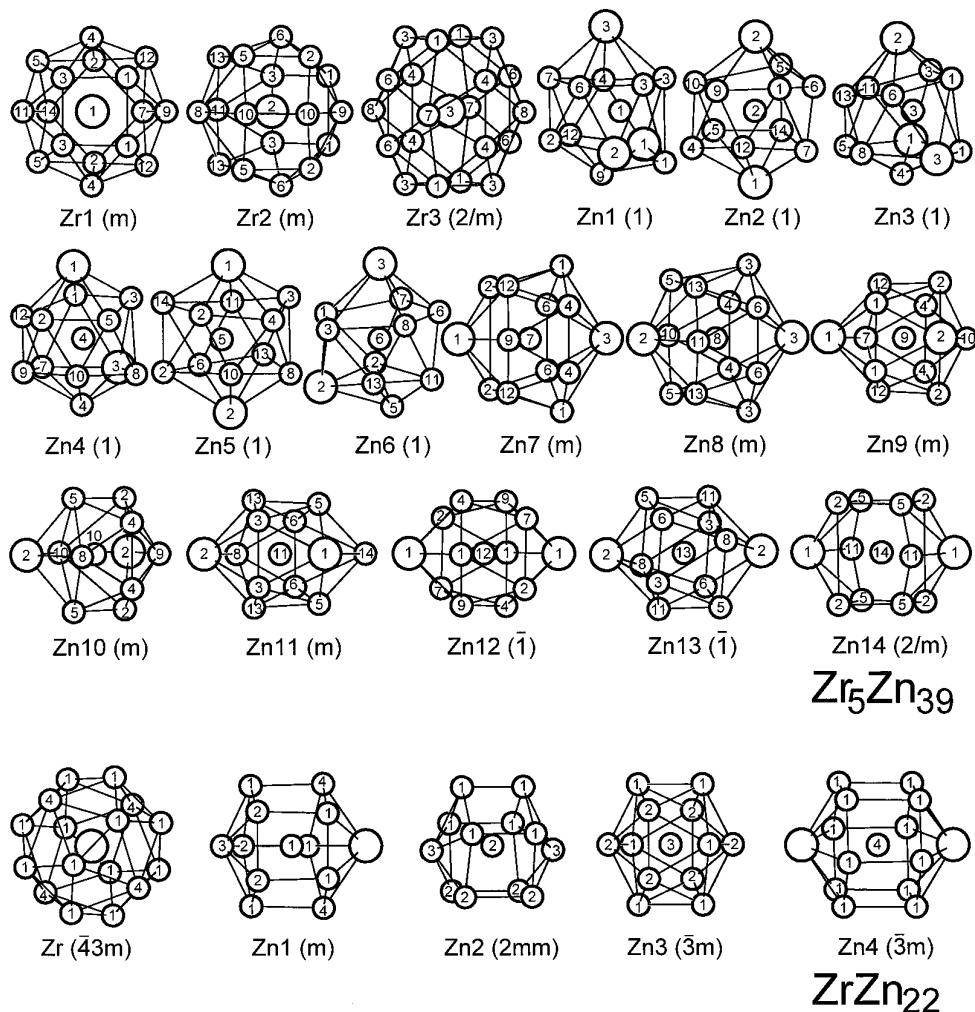


FIG. 5. Coordination polyhedra in the structures of  $Zr_5Zn_{39}$  and  $ZrZn_{22}$ . The numbers correspond to the atom designations. The site symmetries of the central atoms are also indicated.

of  $Zr_5Zn_{39}$  and  $ZrZn_{22}$ . In Figs. 3 and 4 we have marked these voids with the labels V1–V4 and V1–V3, respectively, and in Table 4 we list their positions and distances to the nearest neighbors. Our difference Fourier analyses clearly showed that the positions of these voids are unoccupied in  $Zr_5Zn_{39}$  and  $ZrZn_{22}$ , however, they could be occupied in compounds of related compositions.

This is indeed the case for the structure of  $Ce_5Mg_{41}$  (21), which is closely related to that of  $Zr_5Zn_{39}$ . Both structures consist of similar atomic layers  $ABA'B'$ , as was discussed above for  $Zr_5Zn_{39}$  (Fig. 3). In Fig. 6 we show the layers **A** and **B** of both structures. To facilitate the comparison we have transformed the structure of  $Zr_5Zn_{39}$  from the standard setting  $C2/m$  to the equivalent setting  $I2/m$ . That body-centered space group is a *translationengleiche* subgroup of the group  $I4/m$  adopted by  $Ce_5Mg_{41}$ . It can be seen that the two structures differ only by a few atomic

positions. The atomic layers drawn with broken lines are equal in both structures. Two essential differences occur in the atomic layers drawn with heavy lines. One difference arises through the Mg3 position of  $Ce_5Mg_{41}$  which is entirely unoccupied in  $Zr_5Zn_{39}$ . This site corresponds to the void position designated V1 in Fig. 3 and Table 4. The other difference concerns the Mg1 positions of  $Ce_5Mg_{41}$ . These positions are in part retained as the Zn10 positions of  $Zr_5Zn_{39}$  and in part they are substituted by the Zn14 atoms, whereby one Zn14 position takes the place of two Mg1 positions. As a result two vacancies (V2 in Fig. 3 and Table 4) are formed adjacent to the Zn14 position of  $Zr_5Zn_{39}$ . This lowers the symmetry from  $I4/m$  to  $I2/m$ .

We have suggested previously that the voids in the structures of  $Ti_3Zn_{22}$  and  $TiZn_{16}$  are filled with nonbonding electrons of the zinc atoms (17). This is now supported by the close relationship of the  $Ce_5Mg_{41}$  type and the  $Zr_5Zn_{39}$

structure. The Ce<sub>5</sub>Mg<sub>41</sub> structure was also reported for the compounds Ln<sub>5</sub>Mg<sub>41</sub> (Ln = Pr–Sm) (22, 23) and this indicates that cerium is essentially trivalent in Ce<sub>5</sub>Mg<sub>41</sub>. This is also evident from the cell volume of Ce<sub>5</sub>Mg<sub>41</sub>, which is larger than that of Pr<sub>5</sub>Mg<sub>41</sub>. Therefore the valence electron count for Ce<sub>5</sub>Mg<sub>41</sub> is  $5 \times 3 + 41 \times 2 = 97$  per formula unit (f.u.). For an isotypic compound Zr<sub>5</sub>Zn<sub>41</sub> a valence electron count of  $5 \times 4 + 41 \times 2 = 102$ /f.u. would result. By leaving some of the zinc positions unoccupied the nearly isotypic structure of Zr<sub>5</sub>Zn<sub>39</sub> obtains a valence electron count of  $5 \times 4 + 39 \times 2 = 98$ /f.u. and this is close to the electron count of 97/f.u. for Ce<sub>5</sub>Mg<sub>41</sub>. Thus it seems that the band structures of Zr<sub>5</sub>Zn<sub>39</sub> and Ce<sub>5</sub>Mg<sub>41</sub> have an optimal electron count/f.u. close to 98 or 97. By filling the voids in Zr<sub>5</sub>Zn<sub>39</sub> with additional zinc atoms additional Zn–Zn interactions would need to occur, which on balance would be more antibonding than bonding. By leaving those voids unoccupied the adjacent zinc atoms may place electrons into nonbonding orbitals pointing towards the voids. This is similar to the space requirement of the well-known lone pairs in compounds of the main group elements. The defect structure of Ni<sub>3</sub>Sn<sub>4</sub> as compared to the “filled-up” structure of CoGe (Co<sub>4</sub>Ge<sub>4</sub>) has been rationalized similarly (24).

TABLE 4  
Location and Coordination of Unoccupied Sites □ (voids V)  
in the Structures of Zr<sub>5</sub>Zn<sub>39</sub> and ZrZn<sub>22</sub>

Zr <sub>5</sub> Zn <sub>39</sub> □ <sub>7</sub>		x	y	z
V1	2b	0	1/2	0
V2	4i	0.037	0	0.695
V3	4h	0	0.729	1/2
V4	4g	0	0.762	0
ZrZn <sub>22</sub> □ <sub>17</sub>				
V1	8b	3/8	3/8	3/8
V2	32e	0.283	0.283	0.283
V3	96g	0.310	0.310	0.121
Zr <sub>5</sub> Zn <sub>39</sub> □ <sub>7</sub>	ZrZn <sub>22</sub> □ <sub>17</sub>			
V1 4Zn1 230 pm	V1 6Zn2 195 pm			
4Zn3 226 pm				
	V2 3Zn1 195 pm			
V2 2Zn6 204 pm	3Zn2 195 pm			
1Zn14 204 pm				
1Zn11 233 pm	V3 4Zn1 196 pm			
2Zn2 253 pm	1Zn4 208 pm			
2Zn5 254 pm	1Zn2 209 pm			
1Zn7 254 pm				
V3 2Zn5 192 pm				
2Zn2 193 pm				
2Zn10 233 pm				
1Zn14 233 pm				
V4 2Zn3 203 pm				
2Zn1 204 pm				
1Zr3 204 pm				

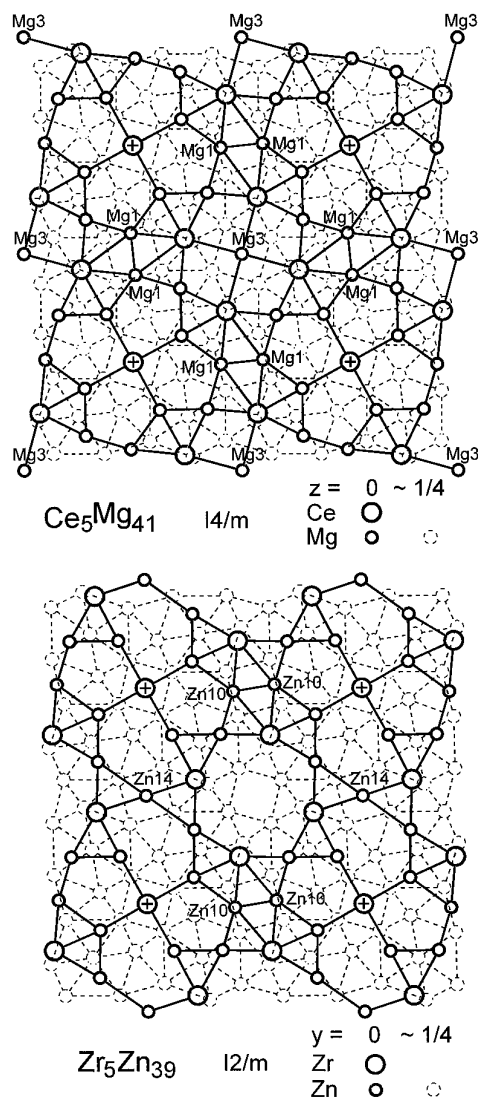


FIG. 6. The crystal structure of Zr<sub>5</sub>Zn<sub>39</sub> in the setting  $I2/m$  as compared to the tetragonal ( $I4/m$ ) structure of Ce<sub>5</sub>Mg<sub>41</sub>. Two corresponding atomic layers of both structures are shown. The origins of the cells are marked by crosses. The Mg3 position of Ce<sub>5</sub>Mg<sub>41</sub> is unoccupied in Zr<sub>5</sub>Zn<sub>39</sub>. Of the four Mg1 pairs, shown in the structure of Ce<sub>5</sub>Mg<sub>41</sub>, two are substituted by a Zn14 atom in Zr<sub>5</sub>Zn<sub>39</sub>.

## ACKNOWLEDGMENTS

We thank Dipl.-Ing. U. Rodewald for the collection of the single-crystal intensity data, Dr. T. Ebel for investigating the magnetic susceptibilities of our samples, Dipl.-Chem. A. Lang for the electrical conductivity measurement, and Mr. K. Wagner for the work at the scanning electron microscope. We appreciate a generous gift of silica tubes by Dr. G. Höfer of the Heraeus Quarzschmelze. We also thank the Alexander von Humboldt Foundation for a stipend to one of us (X.-a. Chen). This work was supported by the Deutsche Forschungsgemeinschaft and the Fonds der Chemischen Industrie.

## REFERENCES

1. P. Chiotti and G. R. Kilp, *Trans. Metall. Soc. AIME* **215**, 892 (1959).
2. W. Rossteutscher and K. Schubert, *Z. Metallkd.* **56**, 730 (1965).
3. P. Pietrokowsky, *Trans. AIME* **200**, 219 (1954).
4. S. C. Abrahams, *Z. Kristallogr.* **112**, 427 (1959).
5. S. Samson, *Acta Crystallogr.* **14**, 1229 (1961).
6. R. C. Weast, Ed., "Handbook of Chemistry and Physics," 58th ed. CRC Press, Palm Beach, FL, 1978.
7. G. M. Sheldrick, "SHELXS-86, A Computer Program for Crystal Structure Determination." Univ. Göttingen, Germany, 1986.
8. B. A. Frenz & Associates, Inc. and Enraf Nonius, 1986.
9. D. T. Cromer and J. B. Mann, *Acta Crystallogr. A* **24**, 321 (1968).
10. D. T. Cromer and D. Liberman, *J. Chem. Phys.* **53**, 1891 (1970).
11. L. M. Gelato and E. Parthé, *J. Appl. Crystallogr.* **20**, 139 (1987).
12. S. Samson, *Acta Crystallogr.* **11**, 851 (1958).
13. S. Samson, *Nature* **195**, 259 (1962).
14. S. Samson, *Acta Crystallogr.* **17**, 491 (1964).
15. S. Samson, *Acta Crystallogr.* **19**, 401 (1965).
16. S. Samson, *Acta Crystallogr.* **23**, 586 (1967).
17. X.-a. Chen, W. Jeitschko, M. E. Danebrock, C. B. H. Evers, and K. Wagner, *J. Solid State Chem.* **118**, 219 (1995).
18. F. C. Frank and J. S. Kasper, *Acta Crystallogr.* **11**, 184 (1958).
19. F. C. Frank and J. S. Kasper, *Acta Crystallogr.* **12**, 483 (1959).
20. C. L. Vold, *Acta Crystallogr.* **14**, 1289 (1961).
21. Q. Johnson and G. S. Smith, *Acta Crystallogr.* **22**, 360 (1967).
22. L. L. Rokhlin, V. V. Kinzhibalo, and N. P. Abrukina, *Izv. Akad. Nauk SSSR. Met.* **5**, 119 (1988).
23. A. Saccone, S. Delfino, G. Borzone, and R. Ferro, *J. Less-Common Met.* **154**, 47 (1989).
24. W. Jeitschko and B. Jaberger, *Acta Crystallogr. B* **38**, 598 (1982).